Journal of Solid State Chemistry **144,** 430–436 (1999)
Article ID jssc.1999.8193, available online at http://www.idealibrary.com on IDEAL®

Electron Diffraction Study of Intercalation Compounds Derived from 1T-MoS_2

F. Wypych,*,[1] C. Solenthaler,† R. Prins,* and Th. Weber*

*Laboratory for Technical Chemistry and †Institute for Metallurgy, Swiss Federal Institute of Technology (ETH), 8092 Zurich, Switzerland

Received September 9, 1998; in revised form February 5, 1999; accepted February 8, 1999

The structure of the intercalation compound $K_{0.7}MoS_2$ as well as of its hydrated ($K_{0.3}(H_2O)_yMoS_2$) and oxidation (1T-MoS_2) derivatives were studied by means of selected area electron diffraction (SAED). All the derivatives are shown to have superstructures related to the structure of 2H-MoS_2. The intercalation compound $K_{0.7}MoS_2$ has a $2a \times 2a$-type superstructure (a = lattice parameter of 2H-MoS_2), whereas the superstructure of the hydrated derivative ($K_{0.3}(H_2O)_yMoS_2$) corresponds roughly to an $a \times a\sqrt{3}$-type. Three domains are present in different orientations, each of which can be related to each other by angles of 60° or 120°. 1T-MoS_2 has an hexagonal $a\sqrt{3} \times a\sqrt{3}$-type superstructure. © 1999 Academic Press

INTRODUCTION

The structure and reactivity of MX_2-type transition metal dichalcogenides ($M = 4$ to 6 group elements, X = S, Se, Te) have been intensively investigated in recent decades (1, 2). This type of compound has a *quasi-bidimensional* structure, which consists of stacks of slabs, where every slab being composed of two layers of chalcogen atoms with a layer of transition metal atoms between them. Stacking of the slabs proceeds along the c axis in the sequence $\{X\text{–}M\text{–}X \cdots X\text{–}M\text{–}X\}$ (where $\cdots$ indicates the van der Waals gap). Whereas the interactions within a slab correspond to chemical bonds, those between two neighboring slabs are due to the much weaker van der Waals forces.

An interesting property of these layered compounds is their ability to accommodate molecular and ionic species in their van der Waals gaps, typically through reversible topotactic redox reactions (1, 2). The electrons, which are required for the reduction of the metal centers, may come from chemical redox reactions or electrochemical processes. Such materials are referred to as intercalation compounds. Intercalation compounds have been used to prepare so-called nanocomposites, in which organic macromolecules are located between the MX_2 layers (3–6). They also provide useful solid-state models for different structural aspects of heterogeneous catalysts, such as for the Co–Mo (7) and the active phase-support interactions (8) in alumina-supported Co–MoS_2 hydrotreating catalysts.

In situ transmission electron microscopy and X-ray diffraction have been widely used to characterize the structure as well as the temperature-dependent phase transitions (9–11) of these intercalation compounds. Microscopic domains have been observed in ternary compounds such as Cu_xNbSe_2, Cu_xNbS_2, and Cu_xTaS_2 (10, 12). The presence of the metal cations in the van der Waals gaps was shown to induce the formation of superstructures or phase transitions in the host lattice.

Our work focuses on structural and electronic properties of intercalation compounds of MoS_2. Whereas the number of intercalation compounds that can be formed from the thermodynamically favored 2H modification is rather small and the respective intercalation compounds are usually unstable (13–15), a number of stable intercalation compounds can be obtained from the metastable 1T-MoS_2 (16, 17).

This study deals with the microscopic structure of the (a, b) plane in the intercalation compound $K_{0.7}MoS_2$ and its hydrated and oxidation derivatives, $K_{0.3}(H_2O)_yMoS_2$ and 1T-MoS_2, respectively. The observed superstructures are related to the structure of 2H-MoS_2.

EXPERIMENTAL

$K_{0.7}MoS_2$ was prepared from K_2MoO_4 by sulfidation with H_2S ($K_2MoO_4 + 4H_2S \rightarrow K_2MoS_4 + 4H_2O$) and subsequent reduction with a 20% H_2/N_2 gas mixture ($2K_2MoS_4 + 3H_2 \rightarrow 2K_{0.7}MoS_2 + 0.6K^0 + K_2S + 3H_2S$). $K_{0.7}MoS_2$ is formed as small hexagonal platelets (16) with an average diameter of 3 mm. Experimental details can be found in Ref. (18).

Washing $K_{0.7}MoS_2$ with water (overall reaction: $K_{0.7}MoS_2 + (x + y)H_2O \rightarrow K_{0.7-x}(H_2O)_yMoS_2 + x/2H_2 + xKOH$) leads to the hydration of the intercalated K^+ cations together with oxidation of molybdenum and

[1] Permanent address: Universidade Federal do Paraná, CP 19081, 81531-990 Curitiba, Pr, Brazil.

0022-4596/99 $30.00

reduction of H_2O. At the beginning of the hydration reaction the pH value is rather high due to the formation of KOH, whereas the $K_{0.3}(H_2O)_yMoS_2$ phase is stabilized at pH = 8 (18). In $K_{0.3}(H_2O)_yMoS_2$, the K^+ cations are located in octahedral van der Waals sites and are surrounded by H_2O molecules, which build a monolayer around the intercalated cations.

1T-MoS_2 was prepared from $K_{0.3}(H_2O)_yMoS_2$ by oxidation with a saturated solution of I_2 in CH_3CN (12 h at room temperature). Depending on the reaction time (i.e., on the extent of oxidation), products with different surface structures can be obtained. For the formation of the final oxidation product, 1T-MoS_2, a reaction time of at least 1 h is required (19). 2H-MoS_2 (99%) was purchased from the Aldrich Co.

The material obtained from the above-mentioned preparation procedures is in the form of very thin, mosaic-like crystallites. We have, therefore, chosen selected-area electron diffraction (SAED) rather than single-crystal X-ray analysis for structural characterization.

SAED measurements were performed with a Philips CM 200 transmission electron microscope (TEM) operating at 200 kV. The intercalation compounds and 1T-MoS_2 decompose upon heating to the thermodynamically favored 2H-MoS_2. Therefore, analysis of the crystallites was done at room temperature ($20 \pm 2^\circ C$). However, the possibility of slight dehydration of the $K_{0.3}(H_2O)_yMoS_2$ intercalation compound in the high vacuum of the microscope cannot be excluded. Due to the natural orientation of the layered materials, the electron beam was applied along the *c* axis of the crystals. The areas of the diffracted samples were 10, 20, or 40 μm.

RESULTS AND DISCUSSION

Prior to the transmission electron diffraction analysis, the samples were characterized by means of conventional analytical methods. Solid-state proton nuclear magnetic resonance (^{1}H-NMR) spectra, obtained from the hydrated phase ($K_{0.3}(H_2O)_yMoS_2$), showed a doublet due to the coordination of H_2O molecules to the intercalated K^+ cations. Obviously, the mobility of the water molecules is unusually high and leads to rotations around the cations and to translational movements within the van der Waals gaps (20, 21).

For the sake of clarity, the SAED patterns are also presented schematically (Figs. 1–7). These consist of bold solid circles, which represent the SAED spots of the 2H-MoS_2 structure and of smaller shaded circles which represent additional spots due to the superstructure of the intercalation compounds. It is important to note that the differences in the size and appearance of the circles are to facilitate the discrimination between these two series of spots in the SAED patterns. In particular, there is no correlation between the size of the circles and the intensities of the spots in the SAED patterns.

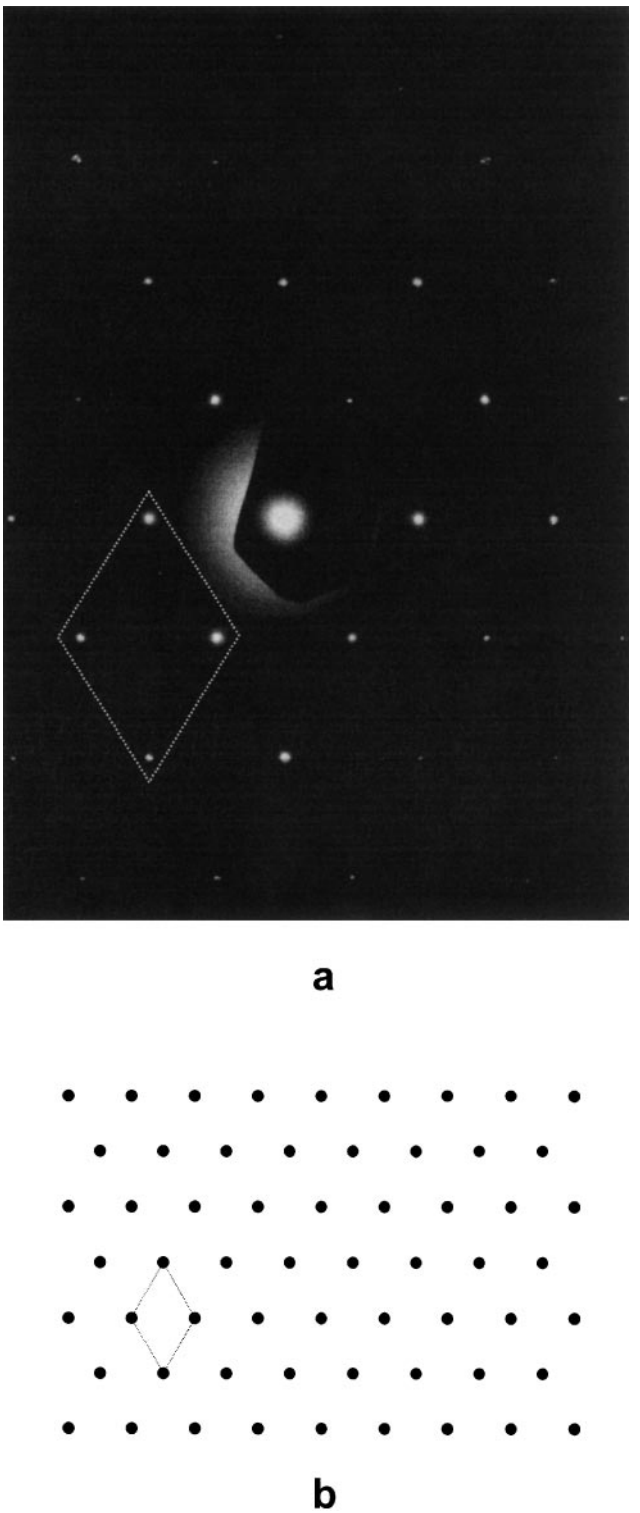

FIG. 1. (a) Measured and (b) schematic SAED pattern of 2H-MoS_2. Diffracted area: 10 μm.

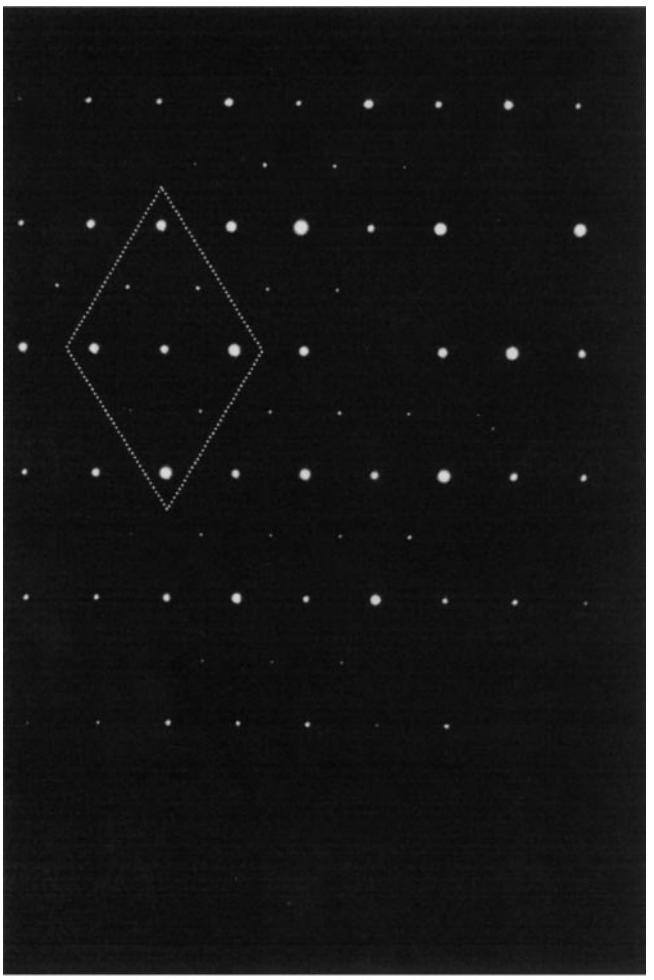

a

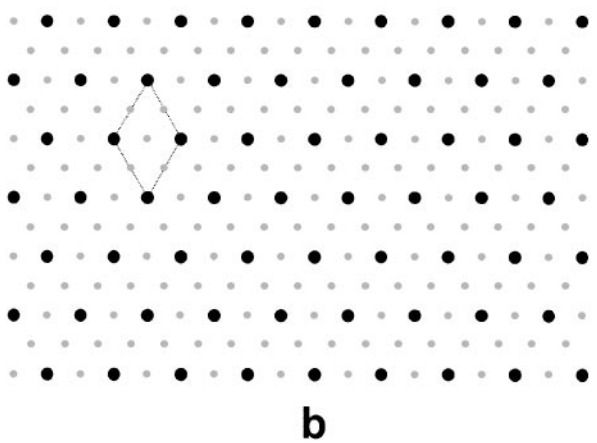

b

FIG. 2. (a) Measured and (b) schematic SAED pattern of the intercalation compound $K_{0.7}MoS_2$. Diffracted area: 10 μm.

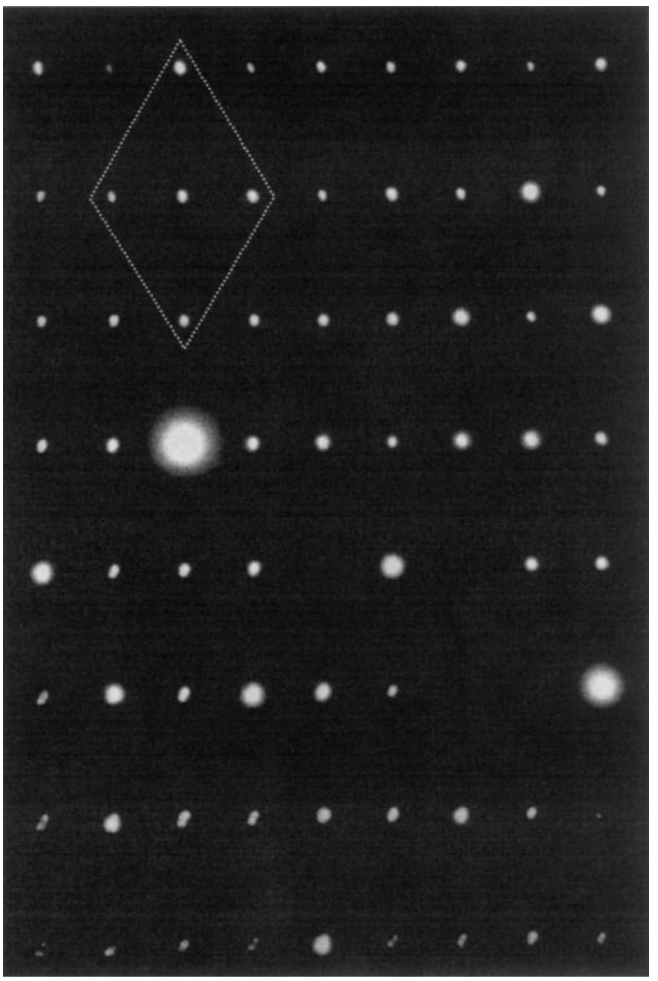

a

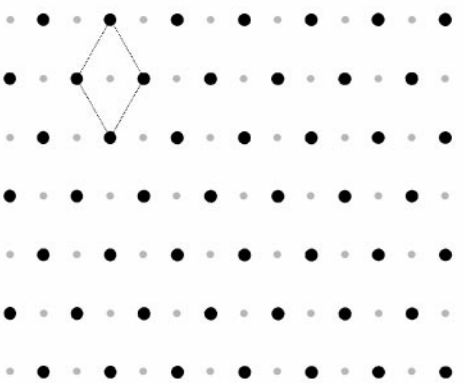

b

FIG. 3. (a) Measured and (b) schematic SAED pattern of the hydrated intercalation compound $K_{0.3}(H_2O)_yMoS_2$. Diffracted area: 10 μm.

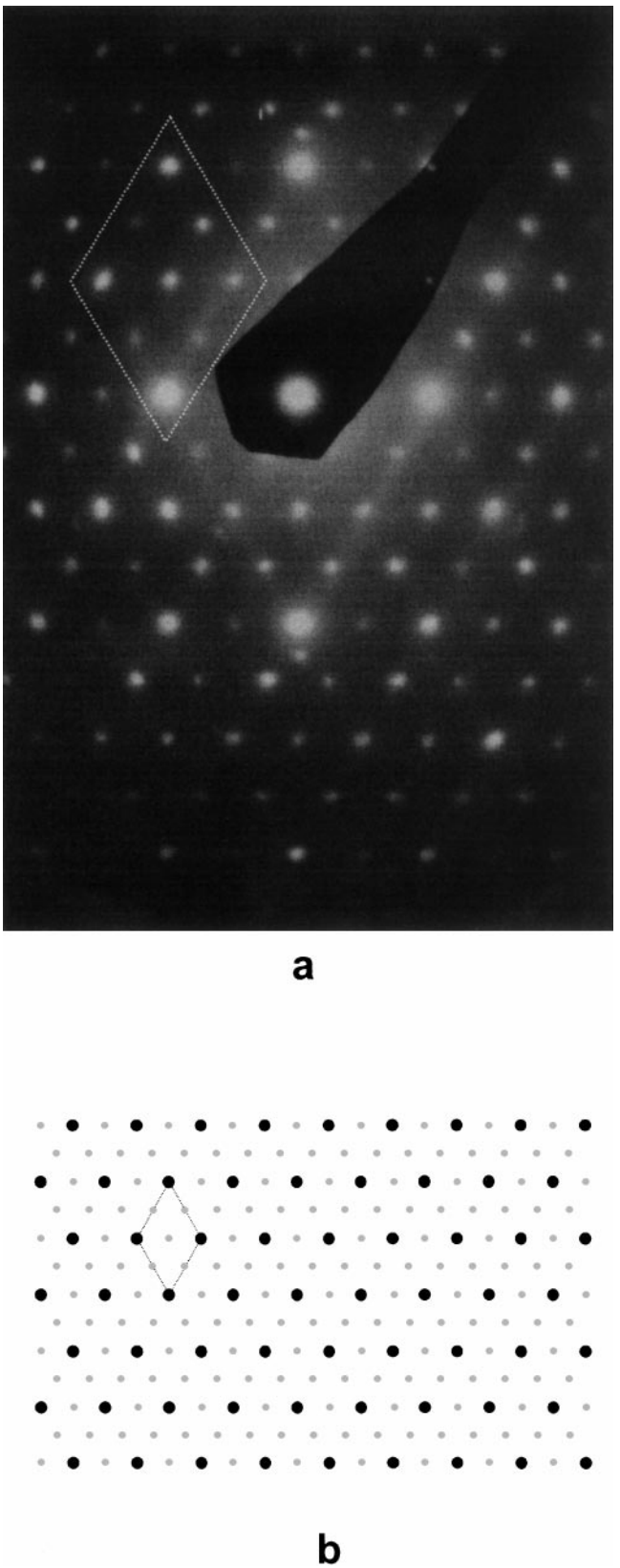

FIG. 4. (a) Measured and (b) schematic SAED pattern of $K_{0.3}(H_2O)_yMoS_2$ showing a larger region (40 μm) of the sample.

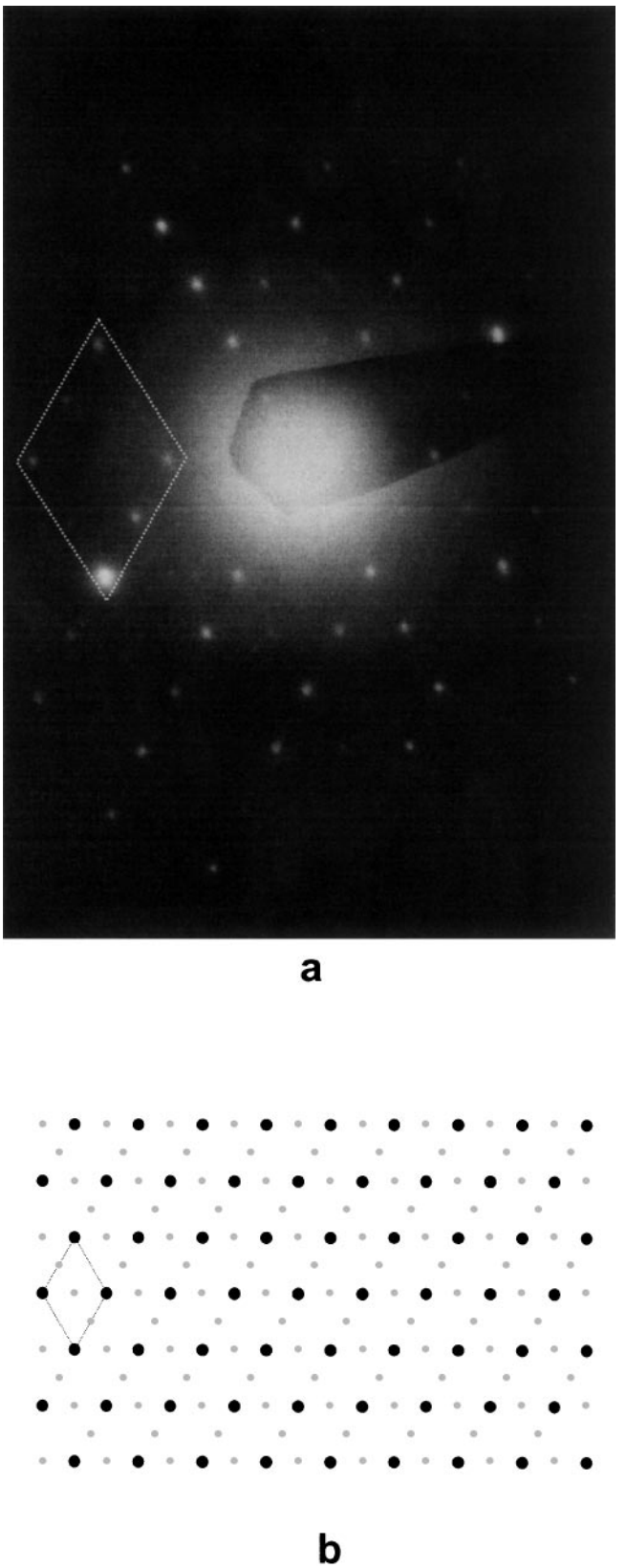

FIG. 5. SAED pattern of an intermediate sample area (20 μm) of (a) $K_{0.3}(H_2O)_yMoS_2$ and (b) its schematic representation.

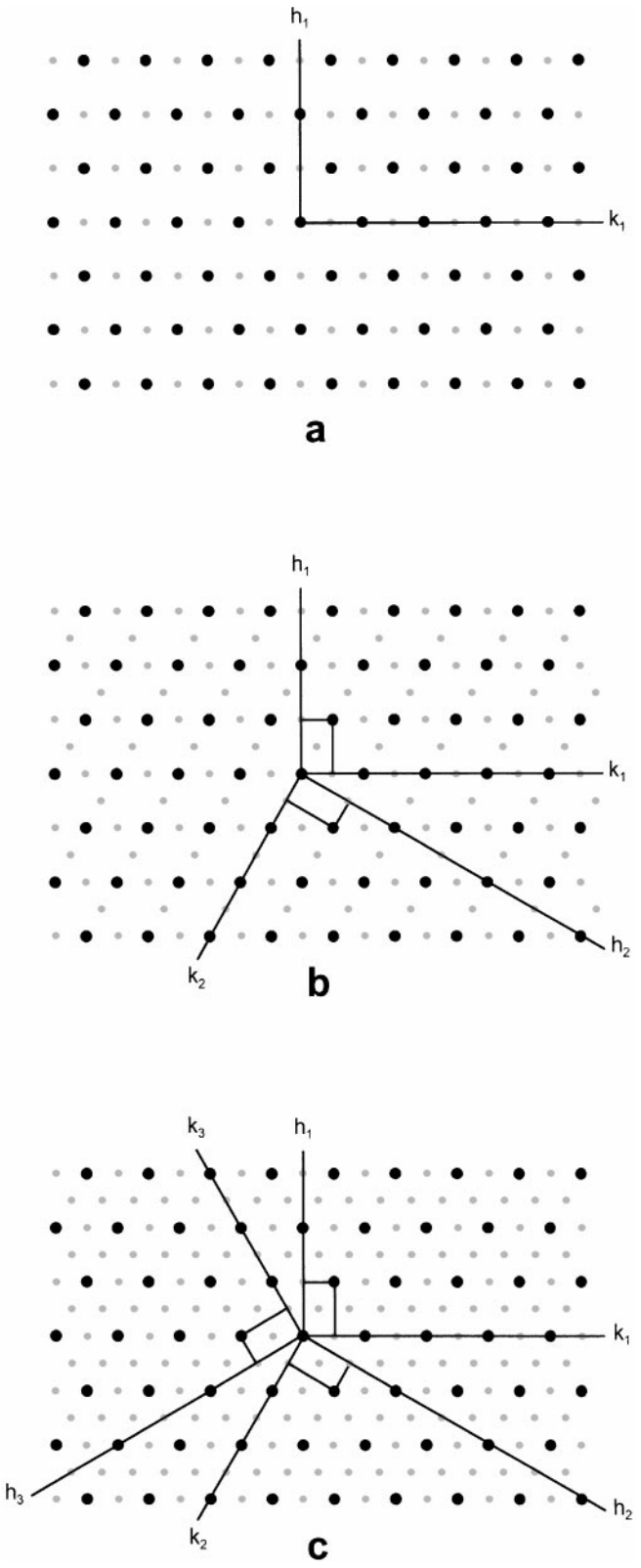

FIG. 6. Scheme of the reciprocal lattice of $K_{0.3}(H_2O)_yMoS_2$: (a) one domain, (b) two domains related by an angle of 60°, and (c) three domains related by angles of 60° and 120°.

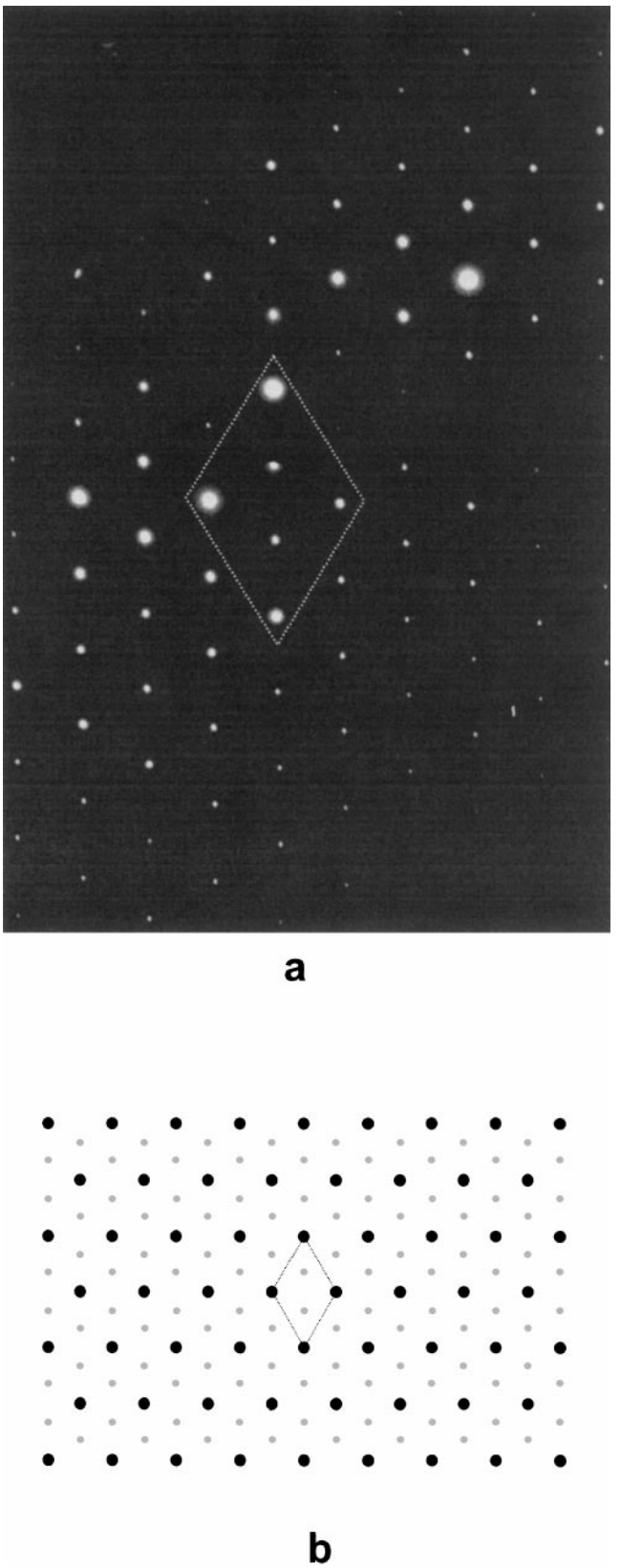

FIG. 7. (a) Measured and (b) schematic SAED pattern of 1T-MoS_2. Diffracted area: 10 μm.

The measured SAED pattern of the binary compound 2H-MoS_2 as well as a schematic presentation of the same are shown in Figs. 1a and 1b. The hexagonal symmetry of 2H-MoS_2, that forms the underlying lattice symmetry of the intercalation compounds, is clearly visible.

The measured SAED pattern of the intercalation compound $K_{0.7}MoS_2$ as well as a schematic presentation of the same are shown in Figs. 2a and 2b. In accordance with preliminary results from a single crystal X-ray diffraction analysis (lattice parameters: $a = 0.660 \pm 0.01$ nm, $b = 0.661 \pm 0.01$ nm, $c = 0.799 \pm 0.03°$, $\alpha = 76.23 \pm 0.2°$, $\beta = 88.3 \pm 0.3°$, $\gamma = 60.26 \pm 0.3°$, space group $P1$ (22)), the SAED pattern clearly shows the $2a \times 2a$-type superstructure of this compound (note that the observed lattice parameters, i.e., $a, b = 0.66$ nm, are slightly higher than the values for an ideal $2a \times 2a$ superstructure, where $2a$ has a value of 2×0.316 nm $= 0.632$ nm). The SAED pattern of this compound, therefore, contains five additional spots due to the superstructure (cf. Fig. 2b).

Corresponding information about the hydrated derivative $K_{0.3}(H_2O)_yMoS_2$ is shown in Figs. 3a and 3b. The SAED pattern contains one additional spot, which suggests an orthorhombic superstructure with respect to 2H-MoS_2. The distances in this compound, as obtained from the electron diffraction pattern, are shorter than those in 2H-MoS_2.

In order to describe these intercalation compounds with respect to the structure of 2H-MoS_2, we compared the lattice parameters of several crystallographic systems. The relationship between the hexagonal (h) and the orthohexagonal (oh) lattices is given by

$$a_{oh} = a_h, \quad b_{oh} = a_h \cdot \sqrt{3} \quad \text{and} \quad c_{oh} = c_h. \qquad [1]$$

Taking the relationship between the real and the reciprocal lattice (labeled with an asterisk) into account, the lattice parameters of the hexagonal and orthohexagonal systems can be described as

$$a_h^* = \frac{2}{a_h \cdot \sqrt{3}} \quad \text{and} \quad a_{oh}^* = \frac{1}{a_{oh}}$$
$$b_h^* = \frac{2}{b_h \cdot \sqrt{3}} \quad \text{and} \quad b_{oh}^* = \frac{1}{b_{oh}} \qquad [2]$$
$$c_h^* = \frac{1}{c_h} \quad \text{and} \quad c_{oh}^* = \frac{1}{c_{oh}}.$$

The relationship between the orthohexagonal and the hexagonal system in the reciprocal lattice can be determined as

$$a_{oh}^* = a_h^* \cdot \frac{\sqrt{3}}{2}, \quad b_{oh}^* = \frac{b_h^*}{2}, \quad c_{oh}^* = c_h^*. \qquad [3]$$

Analysis of the SAED pattern of $K_{0.3}(H_2O)_yMoS_2$ (Fig. 3) showed that the interlayer distances in this phase are not equal to the a and the $a\sqrt{3}$ axis of the 2H-MoS_2 structure. Therefore, the conditions for the orthohexagonal system are not satisfied, and the structure of this compound was initially assumed to be orthorhombic. The following orthorhombic lattice parameters along the (a^*, b^*) plane were defined

$$a_o \sim a_h \cdot \sqrt{3}, \quad b_o \sim a_h \quad \text{and} \quad c_o \sim c_h, \qquad [4]$$

where a_0 is the lattice parameter of the orthorhombic phase, and a_h is the lattice parameter of the hexagonal phase 2H-$MoS_2 = 0.316$ nm (23).

However, looking at a larger area of the same crystal, the resulting electron diffraction pattern shows five additional spots (Fig. 4). These extra spots suggest the existence of a second hexagonal phase with lattice parameters

$$a_{h_1} = 2a_{h_2}, \qquad [5]$$

where a_{h_1} is the lattice parameter of the hexagonal ternary phase $K_{0.3}(H_2O)_yMoS_2$, and a_{h_2} is the lattice parameter of 2H-MoS_2.

Structural studies of ternary derivatives of early transition metal dichalcogenides, such as Cu_xNbS_2 and Cu_xTaS_2 (10, 11), showed that as many as three different domains can be present in one sample, which, of course, has consequences for the respective electron diffraction patterns. Analysis of different parts of the same sample may lead to different SAED patterns, whereas the electron diffraction pattern of a larger part of the sample can be described as a superposition of these different underlying patterns.

In order to determine whether this applies to our problem, we measured another area of the $K_{0.3}(H_2O)_yMoS_2$ sample. The resulting SAED pattern (Fig. 5) shows three additional spots.

If the schematic representations for a first, second, and third domain are superimposed and related to each other by angles of 60° and 120° (Figs. 3, 4, and 5), three new series of spots are seen in every pattern, in addition to the spots resulting from the individual patterns (Fig. 6).

The lattice parameters a and b were obtained from the electron diffraction pattern, whereas the c parameter was obtained from the X-ray powder diffraction pattern. In this case, the intensity of the basal peaks was considerably higher due to the preferential orientation of the layered crystals on the sample holder.

Full indexation was possible only if a monoclinic lattice symmetry was assumed. Therefore, the symmetry of the crystal cannot be orthorhombic.

Assuming that $a = 0.316$ nm (as in 2H-MoS_2 (23)), the lattice parameters are close to the theoretical values as

obtained from Eq. [4]. It should be noted that the actual type of superstructure in the potassium intercalated ternary phase ($K_{0.3}(H_2O)_yMoS_2$) is not due to the ordering of the (hydrated) K^+ cations in the van der Waals gaps but to coordinative distortions of the octahedrally coordinated molybdenum centers (i.e., the [MoS_6] octahedra are not ideally symmetric). These coordination irregularities lead to the formation of a wavy surface structure, as concluded from solid-state proton nuclear magnetic resonance (^{1}H-NMR) (20) and scanning tunneling microscopic measurements (18).

Some of our SAED measurements with $K_{0.3}(H_2O)_yMoS_2$ showed diffuse spots which could not be indexed, although they were evenly distributed over the pattern. They might be the result of a multiple scattering effect of the diffracted beam.

The method described for $K_{0.3}(H_2O)_yMoS_2$ was also used to analyze the microstructure of 1T-MoS_2. The measured SAED pattern of 1T-MoS_2 as well as a schematic presentation of the same are shown in Figs. 7a and 7b. Although the electron diffraction pattern of 1T-MoS_2 is similar to that of the 2H modification (Fig. 1), the presence of two additional spots suggests a hexagonal superstructure, which can be referenced to the 2H-MoS_2 structure

$$a = a_h \cdot \sqrt{3} \quad \text{and} \quad b = b_h \cdot \sqrt{3}, \qquad [6]$$

where a, b are the lattice parameters of 1T-MoS_2, and a_h, b_h are the lattice parameters of 2H-MoS_2.

In this case, the formation of the $a\sqrt{3} \times a\sqrt{3}$-type superstructure is induced by a displacement of the metal centers from their ideal positions in such a way that three Mo centers come closer to each other (trimerization) (24, 25).

CONCLUSIONS

Structural investigation of the intercalation compound $K_{0.7}MoS_2$ by means of SAED showed the presence of a $2a \times 2a$-type superstructure in the (a, b) plane of the compound. In the case of the hydrated derivative, $K_{0.3}(H_2O)_yMoS_2$, three distinct domains, related to each other by angles of 60° and 120°, were observed. Although an analysis of the (a, b) plane in the diffraction pattern of this compound suggested orthorhombic crystal symmetry, this was not confirmed when the X-ray diffraction data were taken into consideration. A complete indexation was accomplished only by lowering the symmetry to the monoclinic system, which is the actual crystalline symmetry of the phase. The monoclinic superstructure can be described with respect to the structure of 2H-MoS_2 as $a \times a\sqrt{3}$, where a is the lattice parameter of the binary phase 2H-MoS_2 ($a = 0.316$ nm (23)).

In 1T-MoS_2, only one kind of superstructure was observed, namely the $a\sqrt{3} \times a\sqrt{3}$-type superstructure. Here, the formation of this type of superstructure is initiated by a trimerization of the Mo centers, as described in Refs. (24) and (25).

ACKNOWLEDGMENT

F. Wypych expresses his thanks to the Department of Chemistry, University of Paraná, for granting him a leave of absence.

REFERENCES

1. R. Schöllhorn, "Intercalation Chemistry" (M. S. Whittingham and A. J. Jacobson, Eds.), p. 315. Academic Press, New York, 1982.
2. W. Müller-Warmuth and R. Schöllhorn (Eds.), "Progress in Intercalation Research." Kluwer, Dordrecht, 1994.
3. M. G. Kanatzidis, R. Bissessur, D. C. De Groot, J.L. Schindler, and C. R. Kannewurf, *Chem. Mater* **5,** 595 (1993).
4. R. Bissessur, M. G. Kanatzidis, J. L. Schindler, and C. R. Kannewurf, *J. Chem. Soc. Chem. Commun.* 1582 (1993).
5. R. Bissessur, J. L. Schindler, C. R. Kannewurf, and M. G. Kanatzidis, *Mol. Cryst. Liq. Cryst.* **245,** 249 (1994).
6. L. Wang, J. Schindler, J. A. Thomas, C. R. Kannewurf, and M. G. Kanatzidis, *Chem. Mater.* **7,** 1753 (1995).
7. K. E. Dungey, M. D. Curtis, and J. E. Penner-Hahn *Chem. Mater.* **10,** 2152 (1998).
8. J. Heising, F. Bonhomme, and M.G. Kanatzidis *J. Solid State Chem.* **139,** 22 (1998).
9. T. J. Hibma, *J. Solid State Chem.* **34,** 97 (1980).
10. R. Ridder, G. van Tendeloo, J. van Landuyt, D. van Dyck, and S. Amelinckx, *Phys. Status Solidi A* **37,** 591 (1976).
11. J. van Landuyt, G. van Tendeloo, and S. Amelinckx, *Phys. Status Solidi A* **26,** 359 (1974).
12. W. Paulus, G. A. Wiegers, A. Meetsma, S. van Smaalen, and J. L. de Boer *Phys. Status Solidi A* **114,** 91 (1989).
13. R. B. Somoano, V. Hadek, A. Rembaum, S. Samson, and J. A. Woollam *J. Chem. Phys.* **62,** 1068 (1975).
14. R. B. Somoano, V. Hadek, and A. Rembaum *J. Chem. Phys.* **58,** 697 (1973).
15. W. Rüdorff, *Chimia* **19,** 489 (1965).
16. F. Wypych and R. Schöllhorn, *J. Chem. Soc. Chem. Commun.* 1386 (1992).
17. F. Wypych, K. Sollmann, and R. Schöllhorn, *Mater. Res. Bull.* **27,** 545 (1992).
18. F. Wypych, Th. Weber, and R. Prins, *Surf. Sci.* **380,** L474 (1997).
19. F. Wypych, Th. Weber, and R. Prins, *Chem. Mater.* **10,** 723 (1998).
20. M. Lobert, W. Müller-Warmuth, H. Katzke, and R. Schöllhorn, *Ber. Bunsenges. Phys. Chem.* **96,** 1564 (1992).
21. V. Alexiev, H. Meyer zu Altenschildesche, R. Prins, and Th. Weber, *Chem. Mater.* submitted for publication.
22. F. Wypych, R. Prins, C. Kronseder, R. Nesper, and Th. Weber, in preparation.
23. K. D. Bronsema, J. L. de Boer, and F. Jellinek, *Z. Anorg. Allg. Chem.* **540,** 15 (1986).
24. C. Rovira and M.-H. Whangbo *Inorg. Chem.* **32,** 4094 (1993).
25. R. Guzmán, J. Morales, and J. L. Tirado, *Inorg. Chem.* **33,** 3164 (1994).